Published in Optics Letters 26, issue 4, 208-210, 2001
which should be used for any reference to this work

Quantitative amplitude and phase measurement by use of a heterodyne scanning near-field optical microscope

Antonello Nesci, René Dändliker, and Hans Peter Herzig
Institute of Microtechnology, University of Neuchâtel, Rue A.-L. Breguet 2, 2000 Neuchâtel, Switzerland

A coherent photon scanning tunneling microscope is presented. The setup employs heterodyne interferometry, allowing both the phase and the amplitude of the optical near field to be measured. Experimental results of measurements on a standing evanescent wave reveal the high resolution that is obtainable with such an approach. In fact we have measured the amplitude and the phase of the near field, with a resolution of 1.6 nm between sample points.

The scanning near-field optical microscope (SNOM) is a powerful instrument for investigating the optical properties of subwavelength structures with high resolution. Many different instrumental techniques have been developed[1,2] to obtain such information. However, most of today's SNOM's measure only intensity. Recently some authors reported measuring phase in the near field with SNOM's,[3,4] in one case with the heterodyne technique.[5] Our main goal is to understand the interaction of light with nanostructures to better determine their shape and optical properties. Essential information on the interaction of light with small structures can be found not only in the intensity but also in the phase of the optical field.[6–8] For this purpose we have developed a coherent SNOM with heterodyne detection for accurate phase measurements.[9] The properties of this instrument are discussed, and we report amplitude and phase measurements of a standing evanescent wave with very high resolution.

The concept of heterodyne interferometry[10] is to introduce a small frequency shift Δf between two interfering beams. As a result of this shift, the interference of the two beams produces an intensity modulation at the beat frequency, $\Delta f = f_1 - f_2$, which is then detected. The setup of the SNOM with heterodyne detection is shown in Fig. 1. The laser is a 150-mW frequency-doubled Nd:YAG diode-pumped solid-state laser ($\lambda = 532$ nm). After separation by a beam splitter (BS), the object and reference beams are shifted in frequency by two acousto-optic modulators (AOM), driven at $f_1 = 40.07$ MHz and $f_2 = 40.00$ MHz. Bringing a commercial atomic-force microscope cantilever[11] fiber probe close to the surface perturbs the field, resulting in propagation in the fiber. This process is called photon scanning tunneling microscopy. The reference and object beams are combined in a fiber coupler, producing a beat signal at 70 kHz, which is detected by a standard silicon photodiode. Since the object power, P_O, is small compared with the reference power, P_R, the coupling ratio of the fiber coupler is chosen to be 90% P_O to 10% P_R. A polarization controller is used to get maximum interference. During measurement, the polarization is stable.

The complex amplitude of the optical field sampled by the fiber tip is given by

$$V(\mathbf{x}, t) = A(\mathbf{x})\exp[i\phi(\mathbf{x})]\exp(i\omega t), \tag{1}$$

where $A(\mathbf{x})$ is the amplitude and $\phi(\mathbf{x})$ is the phase. In common photon scanning tunneling microscopy, only the intensity $I = |A|^2$ is measured. However, because we use heterodyne detection, direct measurement of the amplitude and the phase is possible. Using synchronous detection of the heterodyne signal with a lock-in amplifier, we get two electronic output signals,

$$S(\mathbf{x}) = a(\mathbf{x})\sin\,\phi(\mathbf{x}), \tag{2}$$

$$C(\mathbf{x}) = a(\mathbf{x})\cos\,\phi(\mathbf{x}), \tag{3}$$

where $a(\mathbf{x})$ is proportional to the optical amplitude, $A(\mathbf{x})$, and from which $A(\mathbf{x})$ and $\phi(\mathbf{x})$ can be calculated. Besides the fact that coherent detection allows the optical field phase to be determined, we also get an increased dynamic range. This increase occurs because the amplitude $a(\mathbf{x})$ of the electrical signal is proportional to the amplitude $A(\mathbf{x})$ of the optical field, rather than to the intensity. In addition, we can always get shot-noise-limited detection, even with a photodiode,[12]

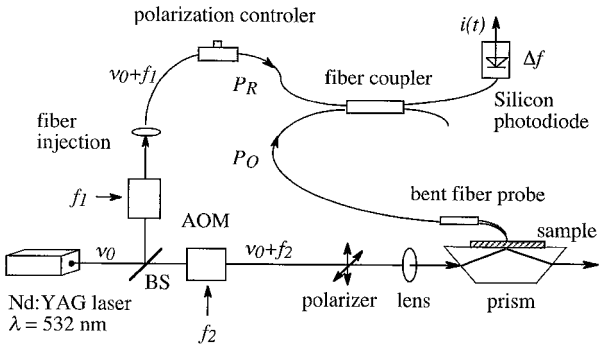

Fig. 1. Photon scanning tunneling microscope with heterodyne detection.

if P_R is chosen to be sufficiently large to overcome the electronic noise. The signal-to-noise ratio is then given by

$$\mathrm{SNR_{dB}} = 10 \log\left(\frac{SP_O}{eB}\right), \tag{4}$$

where S is the spectral sensitivity of the photodiode, e is the electron charge, and B is the bandwidth of the detection. We measured a signal-to-noise ratio of 58 dB for $P_O = 15$ pW and $B = 62.5$ Hz. We determined P_O independently from the same setup (Fig. 1) by blocking the reference beam and measuring the corresponding photodiode current. From Eq. (4) with $S = 0.39$ A/W, $B = 62.5$ Hz, and $P_O = 15$ pW, we get a theoretical signal-to-noise ratio of 58 dB, which is equal to that which was measured.

Near-field amplitude and phase measurements of a standing evanescent-wave field on a prism have also been made. After the first total internal reflection in the prism (with an angle θ_1), the beam is reflected back by an external mirror, creating a standing wave (Fig. 2). In the case of TE polarization, the evanescent field is given by

$$E_y(x,z) = E_1 \exp(-z/z_1)\exp(ikn \sin\theta_1 x) + E_2 \exp(-z/z_2)\exp(-ikn \sin\theta_2 x)\,, \tag{5}$$

where $k = 2\pi/\lambda$ is the wave number, n is the refractive index, E_1 and E_2 are the amplitudes of the two incident waves, and $z_1(\theta_1)$ and $z_2(\theta_2)$ are the penetration depths of the corresponding evanescent waves. If $\theta_1 = \theta_2 = \theta$, we get $z_1 = z_2 = z_0$ and

$$\Lambda = \frac{\lambda}{2n \sin\theta} \tag{6}$$

for the period of the standing wave. In this case the amplitude $A(\mathbf{x})$ and the phase $\phi(\mathbf{x})$ of the sampled field become

$$A(\mathbf{x}) = A_0 \exp(-z/z_0)[1 + m^2 + 2m\cos(2nkx \sin\theta)]^{1/2}, \tag{7}$$

$$\tan\phi(\mathbf{x}) = \frac{1-m}{1+m}\tan(nkx \sin\theta)\,, \tag{8}$$

where the ratio $m = E_1/E_2$ of the incident-field amplitudes has been introduced.

After approaching the fiber with a conventional atomic-force microscope regulated approach, we scanned across the prism surface at constant height. By scanning across the prism surface at constant height, we acquired the amplitude and the phase of the optical field (in TE illumination), as shown in Fig. 3. The period was found to be $\Lambda = 185$ nm. With $\lambda = 532$ nm and $n = 1.5$, we get from Eq. (6) an angle of $\theta = 73°$, which corresponds with the experimental setup. A cross section of another separate measurement in the x direction is shown in Fig. 4. The phase shows the expected π-phase changes for each period of the standing wave, with a spatial resolution of 7.8 nm between sample points. The 2π-phase jumps are due to phase wrapping. We found good agreement with theoretical values obtained from Eqs. (7) and (8), with $m = 0.7$ and $\theta_1 = \theta_2 = 73°$. Figure 5 shows another separate measurement with a step of 1.6 nm between sampling points. We can see that the spatial resolution of the amplitude and phase is given by the sampling steps of 1.6 nm. The measured values correspond very well to the calculations obtained from Eqs. (7) and (8) with $\theta_1 = \theta_2 = 73°$ and $m = 0.78$, which means that the intensity of the

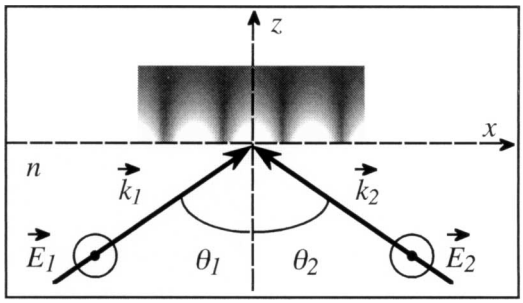

Fig. 2. Standing evanescent wave created by total internal reflection.

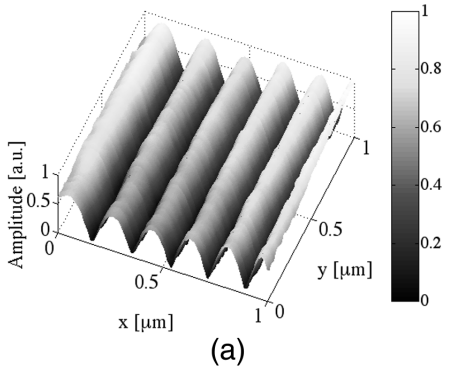

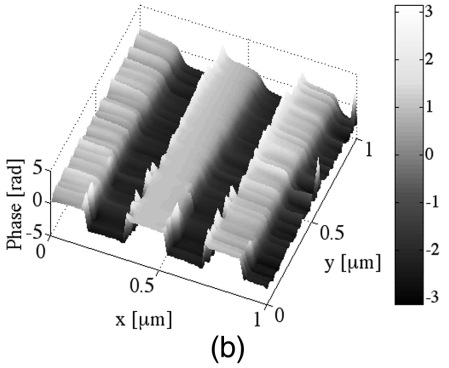

Fig. 3. Measured (a) amplitude and (b) phase of a standing evanescent wave. The scan area is 1 μm by 1 μm.

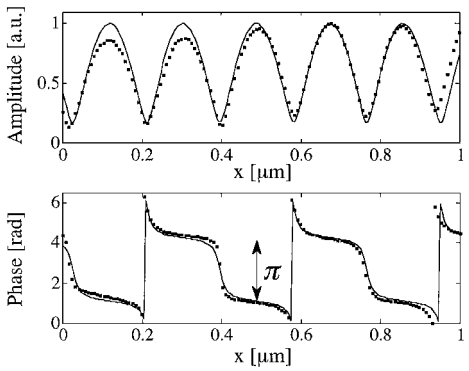

Fig. 4. Cross section of the measured (a) amplitude and (b) phase of the standing evanescent wave. The step is 7.8 nm between sampling points. The solid curves are theoretical calculations ($m = 0.7, \theta_1 = \theta_2 = 73°$).

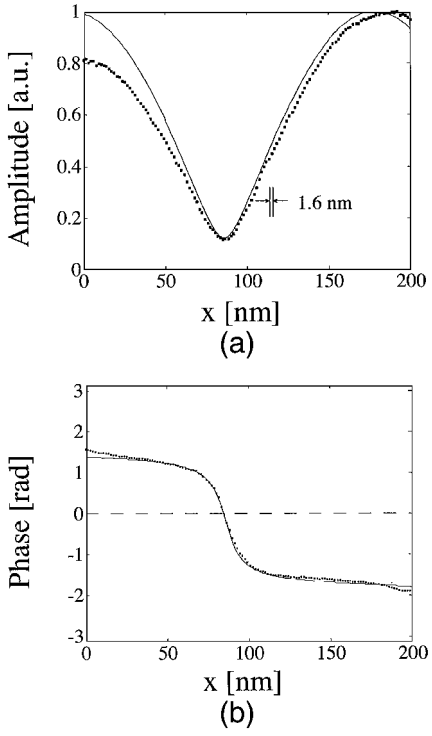

Fig. 5. Measured (a) amplitude and (b) phase of the standing evanescent wave, with a step of 1.6 nm between sampling points. The scan length is 200 nm. The solid curves are theoretical calculations with $\theta_1 = \theta_2 = 73°$ and $m = 0.78$.

backward wave is only ~60% of that of the forward wave. Although the intensity does not go to zero at the nodes of the standing wave, the transition of the phase is very steep (~0.13 rad/nm) around these points, as expected from Eq. (7). Unlike intensity measurements, in coherent detection, the finite width of the fiber tip (~30 nm in our case) averages the field amplitude, and therefore for $m = 1$ the measured amplitude would go to zero.

We have demonstrated that scanning near-field optical microscopy with coherent (heterodyne) detection is a powerful method for measuring both the amplitude and the phase of an optical field on the nanometer scale. Heterodyne SNOM also has a larger dynamic range than standard methods, since it measures the amplitude rather than the intensity, and one can always obtain shot-noise-limited detection by choosing a sufficiently large reference power. We have presented amplitude and phase measurements of a standing evanescent wave, with a resolution of 1.6 nm between sample points. The results are in very good agreement with the theory. These test measurements are very useful because the prism surface is flat, meaning that topography perturbs neither the motion of the probe nor the optical signal. Changes of amplitude and phase around phase singularities can be observed with high resolution, since the finite width of the fiber tip averages the field amplitude rather than the intensity. In future work we intend to measure fields close to micrometer-scale diffraction gratings to characterize our instrument.

The authors thank Peter Blattner and Martin Salt for helpful discussions. This research was supported by the Swiss National Science Foundation. A. Nesci's e-mail address is antonello.nesci@unine.ch.

References

1. M. A. Paesler and P. J. Moyer, *Near Field Optics* (Wiley, New York, 1996).
2. M. Ohtsu and H. Hori, *Near-Field Nano-Optics* (Kluwer Academic, Dordrecht, The Netherlands, 1999).
3. M. Vaez-Iravani and R. Toledo-Crow, Appl. Phys. Lett. **62,** 1044 (1993).
4. P. L. Phillips, J. C. Knight, J. M. Pottage, G. Kakarantzas, and P. St. J. Russell, Appl. Phys. Lett. **76,** 541 (2000).
5. M. L. M. Balistreri, J. Korterik, K. Kuipers, and N. van Hulst, Phys. Rev. Lett. **85,** 294 (2000).
6. M. Tozeck and H. J. Tiziani, Opt. Commun. **138,** 365 (1997).
7. R. Dändliker, P. Blattner, and H. P. Herzig, Proc. SPIE **3749,** 74 (1999).
8. P. Blattner, C. Rockstuhl, H. P. Herzig, and R. Dändliker, in *Nanoscale Optics*, Vol. 25 of EOS Topical Meeting Digests Series (European Optical Society, Paris, 2000), p. 68.
9. A. Nesci, P. Blattner, H. P. Herzig, and R. Dändliker, in *Nanoscale Optics*, Vol. 25 of EOS Topical Meeting Digests Series (European Optical Society, Paris, 2000), p. 52.
10. B. Saleh and M. Teich, *Fundamental of Photonics* (Wiley, New York, 1991), pp. 907–910.
11. K. Lieberman, A. Lewis, G. Fish, S. Shalom, T. M. Jovin, A. Schaper, and S. R. Cohen, Appl. Phys. Lett. **65,** 648 (1994).
12. J.-F. Willemin and R. Dändliker, J. Acoust. Soc. Am. **83,** 787 (1988).